Self-Induced Oscillations in an Optomechanical System Driven by Bolometric Backaction

Constanze Metzger,[3,2] Max Ludwig,[1,2] Clemens Neuenhahn,[1,2] Alexander Ortlieb,[2] Ivan Favero,[4,2] Khaled Karrai,[2] and Florian Marquardt[1,2]

[1]*Arnold-Sommerfeld Center for Theoretical Physics, Ludwig-Maximilians-Universität München, Munich, Germany*
[2]*Center for NanoScience and Department of Physics, Ludwig-Maximilians-Universität München, Munich, Germany*
[3]*Department of Electrical and Computer Engineering, Boston University, Boston, Massachusetts 02215, USA*
[4]*Laboratoire Materiaux et Phénomènes Quantiques, Université Paris Diderot et CNRS, UMR 7162, Bâtiment Condorcet, 75205 Paris Cedex 13, France*

(Received 27 November 2007; published 26 September 2008)

We have explored the nonlinear dynamics of an optomechanical system consisting of an illuminated Fabry-Perot cavity, one of whose end mirrors is attached to a vibrating cantilever. The backaction induced by the bolometric light force produces negative damping such that the system enters a regime of nonlinear oscillations. We study the ensuing attractor diagram describing the nonlinear dynamics. A theory is presented that yields quantitative agreement with experimental results. This includes the observation of a regime where two mechanical modes of the cantilever are excited simultaneously.

DOI: 10.1103/PhysRevLett.101.133903 PACS numbers: 42.65.−k, 05.45.−a, 07.10.Cm, 85.85.+j

Micro- and nanomechanical systems have become a focus of research [1], with the goals ranging from ultrasensitive measurements to fundamental tests of quantum mechanics. Optomechanical systems are particularly promising, where the interaction of light circulating in an optical cavity with a mechanical system like a cantilever is exploited. This produces a variety of effects, including a modification of the mechanical spring constant [2–7], bistability [8,9], optomechanical cooling, and parametric instability. Recent experiments have made impressive progress in cooling [5,6,10–15], which may ultimately lead to the mechanical ground state [16,17]. The opposite regime is of equal interest, where the mechanical Q factor is enhanced due to the backaction of light-induced forces and a parametric instability arises, driving the system into self-sustained oscillations [2,18–26]. The same physics is also found in other systems as diverse as a driven LC circuit [27], a superconducting single-electron transistor coupled to a nanobeam [28–30], or cold atoms in an optical lattice [31]. Although the basic instability has been observed by now in a number of experiments [20–23,25,26,32], it was recently realized theoretically [24] that the nonlinear dynamics of this system can become highly nontrivial, leading to an intricate attractor diagram. We present an experiment that traces this diagram and offer a detailed analysis and comparison against theory. As an unexpected feature, we observe the simultaneous excitation of several mechanical modes of the cantilever, leading to coupled nonlinear dynamics. The system studied here is dominated by bolometric forces (i.e., light absorption deflecting the bimorph cantilever) and may inspire future studies of the analogous attractor diagram in radiation-pressure-dominated setups (such as [22,23]).

Experimental setup.—We employ the setup displayed in Fig. 1. The light of a 633 nm monomode HeNe laser is coupled into a single mode fiber and passes through a Faraday isolator (35 dB suppression). The fiber end inside a vacuum chamber (at 5×10^{-6} mbar) was polished and coated with a reflecting gold layer of 30 nm (yielding a theoretical reflectivity of 70%) to form the first cavity mirror. The sample is a gold-coated atomic force microscopy cantilever acting as a micromirror, with length 223 μm, thickness 470 nm, width 22 μm, spring constant $K = 0.01$ N/m, and a gold layer of 42 nm evaporated on one side only. The cantilever's fundamental mechanical mode has a frequency of $\omega_1 = 2\pi \times 8.7$ kHz and a damping rate of $\Gamma_1 = 30$ Hz. A simulation of the silicon-gold bilayer system gave a reflectivity of 91% for a wavelength of 633 nm. The divergent beam is sent through a microscope setup consisting of two identical lenses, yielding a

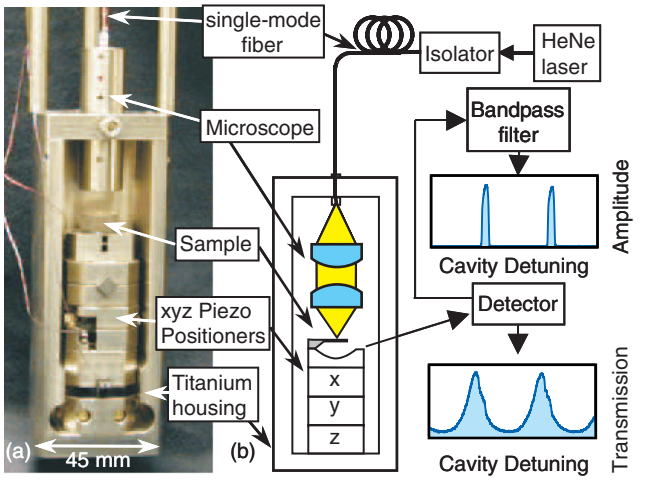

FIG. 1 (color online). The experimental setup. The light inside the optical cavity is focused onto a cantilever, where it exerts a force. Both the transmitted light intensity and its sidebands at the cantilever frequency are recorded (Transmission and Amplitude, respectively).

Gaussian focus on the sample with a $1/e^2$ diameter of 6 μm. The cantilever has been mounted on an xyz piezo stepper positioner block [33], such that it can be placed at the microscope's focal point, which was chosen near the end of the cantilever, at about 3/4 of its length. The finesse of the cavity defined by the sample and the fiber end was found to be $F \approx 4.5$. The transmitted intensity is measured with a Si photodiode behind the cantilever.

Theoretical model.—The dynamics of the cantilever is described by the equation of motion of a damped oscillator, driven by light-induced forces:

$$\ddot{x} = -\omega_1^2(x - x_0) - \Gamma_1\dot{x} + (F^{\mathrm{rad}} + F^{\mathrm{bol}})/m_1. \quad (1)$$

Here $x(t)$ is the cantilever deflection observed at the laser spot. For now, we focus on the motion of the first mechanical mode (with effective mass m_1, frequency ω_1, and damping rate Γ_1) and study higher-order modes below. The cavity is assumed to be in resonance with the laser at $x = 0$, while the mechanical equilibrium position x_0 is controlled by the piezo positioner. The radiation-pressure force F^{rad} is set by the power I circulating inside the cavity: $F^{\mathrm{rad}}/m_1 = \mathcal{P}I$. For an ideally reflecting mirror, we have $\mathcal{P} = (m_1 c)^{-1}$, although in practice $\mathcal{P}$ has to be treated as a fit parameter. The bolometric force F^{bol} arises due to light being absorbed. It is enhanced by a factor Λ over F^{rad} and is retarded due to the finite time of thermal conductance τ (where θ is proportional to the change in temperature):

$$F^{\mathrm{bol}}/m_1 = \Lambda\mathcal{P}\int_{-\infty}^{t}\frac{dt'}{\tau}e^{-(t-t')/\tau}I(t') \equiv \Lambda\mathcal{P}\theta(t). \quad (2)$$

In the present low-finesse setup, the intensity reacts instantaneously to the motion, $I(t) = I[x(t)]$, and the Fabry-Perot resonances overlap: $I[x(t)]/I_{\max} = \{1 + (2F/\pi)^2 \sin[\frac{2\pi}{\lambda}x(t)]^2\}^{-1}$, where $I_{\max}$ is the peak circulating power. In contrast to Ref. [24], the time lag τ of the bolometric force is crucial.

Self-induced oscillations.—Time-retarded forces, produced by the backaction of the light onto the moving cantilever, induce an effective optomechanical damping rate [2,4,16–18,24], which can become negative. Then the system may show a Hopf bifurcation towards self-induced oscillations [24], which (for the present parameters) are sinusoidal to a very good approximation: $x(t) = \bar{x} + A\cos(\omega_1 t)$. The nonlinear dynamics can be characterized by the amplitude A and offset $\bar{x}$. From these we obtain the experimentally observed light intensity $I(t)$. In steady state, the average force and total power input (including both mechanical friction and light-induced effects) must balance to zero, i.e., $\langle\ddot{x}\rangle = 0$ and $\langle\ddot{x}\,\dot{x}\rangle = 0$, where $\langle\ldots\rangle$ denotes the time average. Inserting Eq. (1), we obtain the power balance equation:

$$\mathcal{P}\langle\dot{x}[I(t) + \Lambda\theta(t)]\rangle = \Gamma_1\langle\dot{x}^2\rangle. \quad (3)$$

The radiation pressure does not contribute: $\langle\dot{x}I\rangle = 0$, since $\dot{x}I[x(t)]$ is antisymmetric in time. Equation (3) yields

$$\frac{\Gamma_1}{\mathcal{P}} = \frac{-\Lambda}{A\omega_1\pi}\frac{\omega_1\tau}{(\omega_1\tau)^2 + 1}\int_0^{2\pi}d\varphi I[\bar{x} + A\cos\varphi]\cos\varphi. \quad (4)$$

The force balance condition $\omega_1^2(\bar{x} - x_0) = \mathcal{P}(\langle I\rangle + \Lambda\langle\theta\rangle)$ gives us $\bar{x} = \bar{x}(x_0, A)$:

$$\bar{x} - x_0 = \frac{(1 + \Lambda)\mathcal{P}}{2\pi\omega_1^2}\int_0^{2\pi}d\varphi I[\bar{x} + A\cos\varphi]. \quad (5)$$

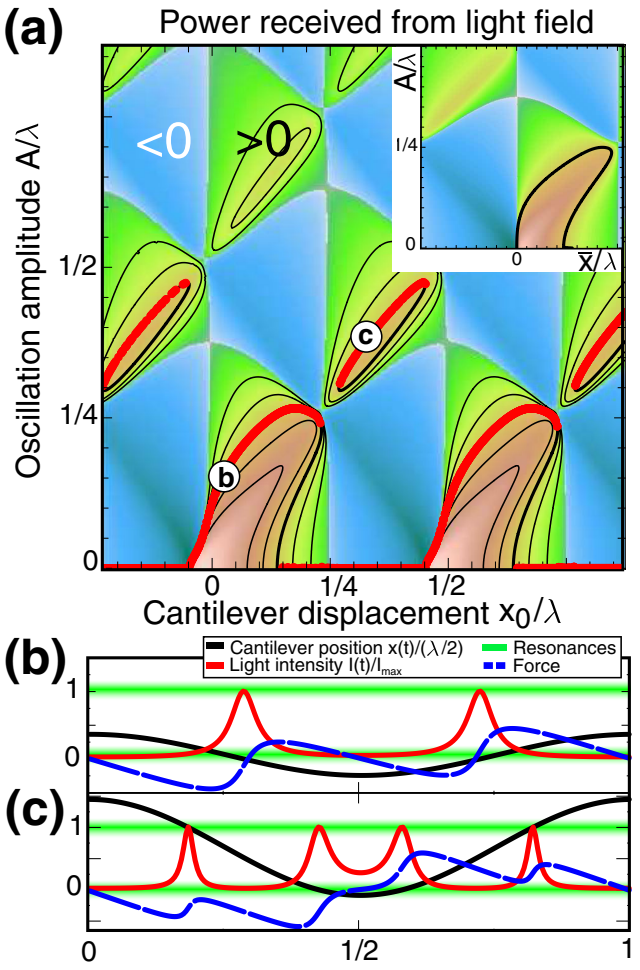

FIG. 2 (color online). Attractor diagram. (a) Amplitude A of self-induced oscillations vs cantilever equilibrium position x_0. The color scale displays the net power fed into the cantilever from the radiation field, i.e., the right-hand side of Eq. (4). Contour lines indicate possible oscillation amplitudes (attractors) for various damping constants Γ_1. Red dots stem from numerical simulations, for the experimental value of Γ_1 (and a laser input power of $I = 0.3I_0$). The inset shows the same plot as a function of $(A, \bar{x})$ instead of (A, x_0). (b),(c) Whenever $x(t)$ (thick black line) passes through the optical resonances (green bars), the light intensity (red line) displays spikes, leading to delayed increases in the radiation force (dashed blue line), which was plotted as $(\theta - \bar{\theta}) \times 200$. Plots (b) and (c) correspond to the positions indicated in the attractor diagram (a).

Attractor diagram.—Using Eqs. (4) and (5), one obtains solutions $(\bar{x}, A)$ which can be visualized in attractor diagrams, like the one shown in Fig. 2. The color scale encodes the power input due to the light-induced forces [right-hand side of Eq. (4)], as a function of x_0 and A. The solution of Eq. (4) for various values of $\Gamma_1/\mathcal{P}$ then corresponds to contour lines of this function. Apart from the expected $\lambda/2$ periodicity in the detuning x_0, the main feature is the appearance of multiple solutions for A at a given x_0 ("dynamical multistability"). The deviation between $\bar{x}$ and x_0 [see Eq. (5)] leads to a distortion of the diagram (inset in Fig. 2). This effect grows with increasing input power, finally leading to multiple solutions for $\bar{x}(x_0, A)$.

Comparison of theory and experiment.—In the experiment, the detuning x_0 and the input power I_{in} are varied, while the transmitted light intensity is measured. This is compared to the time-averaged circulating power $\langle I(t)\rangle$ obtained from the theory. As soon as the oscillations set in, $I(t)$ is modulated at ω_1. A very helpful feature of this system is that the amplitude A is directly proportional to the first harmonic of the light intensity: $\tilde{I}_1 = \frac{1}{T} \times \int_0^T dt \cos(\omega_1 t) I(t)$, where $T = 2\pi/\omega_1$. From Eq. (4), we see that $A = -2(\Lambda \mathcal{P}/\omega_1 \Gamma)\omega_1 \tau [1 + (\omega_1 \tau)^2]^{-1} \tilde{I}_1$. This relation is true only in steady state (on the attractors), but then it is valid even when the motion sweeps across several optical resonances. Experimentally, $\tilde{I}_1$ is obtained by sending the photodetector signal through a narrow bandpass filter (100 Hz) centered at the frequency ω_1.

Theoretical and experimental curves for the average intensity ("transmission") and the amplitude are shown in Fig. 3, for different input powers. We have used $F \approx 4.5$ (from a fit at low input power), $\Lambda = 3950$, and $\omega_1 \tau = 39$ (obtained independently). The conversion factor between experimental input power and the force on the cantilever was found to be $\mathcal{P} I_0 = 0.0775\ \text{m/s}^2$, by fitting to the data at intermediate power (the same was done for the rescaling of theoretical and experimental transmission intensity). The maximum laser power $I_0 = 1.3$ mW is estimated to yield 500 μW circulating in the cavity on resonance.

At the lowest power displayed in Fig. 3, self-oscillations have just set in, and the transmission curve shows a striking asymmetry. At higher input powers, the multistability predicted by the attractor diagram (Fig. 2) leads to hysteresis effects.

Beginning at $I_{\text{in}} = 0.57 I_0$, a second interval of self-oscillatory behavior appears to the *left* of the resonance, growing stronger and wider with increasing laser power. This initially unexpected result may be explained by the influence of higher mechanical modes. These may be excited by the radiation as well, leading to coupled (multimode) nonlinear dynamics. Thus, we have to take into account the second mode as well:

$$\ddot{x}_i = -\omega_i^2 x_i - \Gamma_i \dot{x}_i + F_i^{\text{bol}}[x(t)]/m_i, \qquad (6)$$

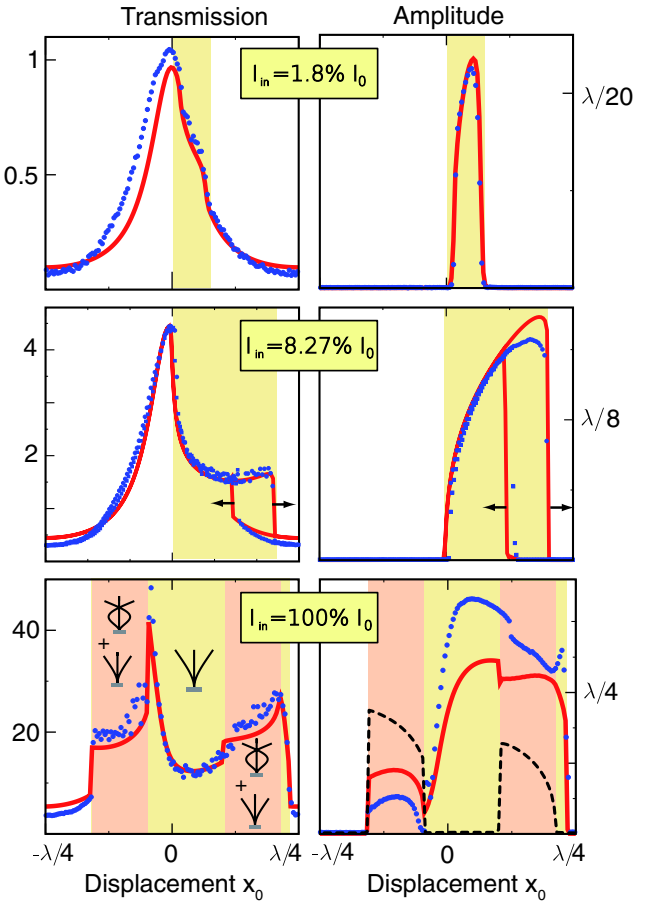

FIG. 3 (color online). Experiment vs theory. The transmitted light intensity (left) and the amplitude of self-induced cantilever oscillations (right), from a numerical simulation (red full curves) and from the experiment (blue data points), at increasing input power levels (top to bottom). Theoretical transmission curves display the (rescaled) time-averaged circulating light intensity from the simulation. Amplitude curves are obtained from the sidebands in the intensity (see main text). For clarity, the hysteresis observed upon sweeping x_0 has been shown only in the middle panel. The region of instability (shaded interval) grows with increasing input power. Simultaneous self-induced oscillations of the first two mechanical modes set in at the highest power displayed (in the two intervals indicated in the plot). The calculated amplitude of the second mode is shown as a dashed line.

where x_i denotes the coordinate of the ith mechanical mode with frequency ω_i, mechanical damping rate Γ_i, and effective mass m_i ($\omega_1/2\pi = 8.7$ kHz, $\omega_2/2\pi = 60$ kHz, $\Gamma_1 = 30.0$ Hz, and $\Gamma_2 = 150$ Hz). The total displacement is $x(t) = x_0 + x_1(t) + x_2(t)$. The mechanical modes are now coupled indirectly by the bolometric force, while radiation pressure is negligible. For the present setup, this force changes sign when going to the second mode. Choosing $F_2^{\text{bol}} m_1 / F_1^{\text{bol}} m_2 = -28.8$ as an adjustable parameter, we have found the numerical simulation of (6) to be in good agreement with the experiment (Fig. 3). We

note that the relation between the measured "amplitude," i.e., first harmonic $\tilde{I}_1$, and the actual amplitude A_1 no longer holds exactly in this regime.

At maximum laser power, there are two intervals with simultaneous excitation of both modes (indicated in Fig. 3). The onset of such a regime at $x_0 \approx \lambda/8$ can be interpreted as follows: Taking into account $F_2^{\mathrm{bol}}/F_1^{\mathrm{bol}} < 0$, we see that the second mode gains its energy from dipping into the resonance at $x = \lambda/2$, while the first is still provided with energy due to the resonance at $x = 0$. Numerical evidence shows that the motion consists of sinusoidal oscillations in $x_{1,2}$, of nearly constant amplitudes and without phase locking (for the parameters explored here). Thus $x(t) \approx x_0 + \sum_{i=1}^{2}[A_i + \delta A_i(t)] \times \cos(\omega_i t + \phi_i)$, where $\delta A_i(t)/A_i \ll 1$ and the ϕ_i are arbitrary phases. Higher input powers will lead to excitations of additional modes, and the system might go into a chaotic regime.

Conclusions.—We have analyzed the nonlinear dynamics of an optomechanical system by measuring and explaining its attractor diagram. The comparison with theory has revealed the onset of multimode dynamics at large power, with two mechanical modes of the cantilever participating in the radiation-driven self-sustained oscillations. These effects could find applications in highly sensitive force or displacement detection [24]. In the future, it would be interesting to observe the attractor diagram in systems of a high optical finesse [22,23], the self-excitation of subwavelength mechanical resonators inside a cavity [15,34], and quantum nonlinear dynamics in optomechanical systems [35].

We acknowledge support by the Nanosystems Initiative Munich (NIM), an Emmy-Noether grant of the DFG (F. M.), and the A. v. Humboldt Foundation (I. F.).

[1] K. C. Schwab and M. L. Roukes, Phys. Today, No. 7, 36 (2005).
[2] V. Braginsky and A. Manukin, Sov. Phys. JETP **25**, 653 (1967).
[3] M. Vogel, C. Mooser, K. Karrai, and R. J. Warburton, Appl. Phys. Lett. **83**, 1337 (2003).
[4] C. Höhberger-Metzger and K. Karrai, Nature (London) **432**, 1002 (2004).
[5] O. Arcizet, P. F. Cohadon, T. Briant, M. Pinard, and A. Heidmann, Nature (London) **444**, 71 (2006).
[6] T. Corbitt *et al.*, Phys. Rev. Lett. **98**, 150802 (2007).
[7] M. Hossein-Zadeh and K. J. Vahala, Opt. Lett. **32**, 1611 (2007).
[8] A. Dorsel, J. D. McCullen, P. Meystre, E. Vignes, and H. Walther, Phys. Rev. Lett. **51**, 1550 (1983).
[9] P. Meystre, E. M. Wright, J. D. McCullen, and E. Vignes, J. Opt. Soc. Am. B **2**, 1830 (1985).
[10] C. Höhberger-Metzger and K. Karrai, Nature (London) **432**, 1002 (2004).
[11] D. Kleckner and D. Bouwmeester, Nature (London) **444**, 75 (2006).
[12] S. Gigan *et al.*, Nature (London) **444**, 67 (2006).
[13] A. Schliesser, P. Del'Haye, N. Nooshi, K. J. Vahala, and T. J. Kippenberg, Phys. Rev. Lett. **97**, 243905 (2006).
[14] I. Favero *et al.*, Appl. Phys. Lett. **90**, 104101 (2007).
[15] J. D. Thompson, B. M. Zwickl, A. M. Jayich, F. Marquardt, S. M. Girvin, and J. G. E. Harris, Nature (London) **452**, 900 (2008).
[16] F. Marquardt, J. P. Chen, A. A. Clerk, and S. M. Girvin, Phys. Rev. Lett. **99**, 093902 (2007).
[17] I. Wilson-Rae, N. Nooshi, W. Zwerger, and T. J. Kippenberg, Phys. Rev. Lett. **99**, 093901 (2007).
[18] V. B. Braginsky, A. B. Manukin, and M. Y. Tikhonov, Sov. Phys. JETP **31**, 829 (1970).
[19] V. B. Braginsky, S. E. Strigin, and S. P. Vyatchanin, Phys. Lett. A **287**, 331 (2001).
[20] K. Kim and S. Lee, J. Appl. Phys. **91**, 4715 (2002).
[21] C. Höhberger and K. Karrai, in *Proceedings of the 4th IEEE Conference on Nanotechnology, 2004* (IEEE, New York, 2004), p. 419.
[22] T. Carmon, H. Rokhsari, L. Yang, T. J. Kippenberg, and K. J. Vahala, Phys. Rev. Lett. **94**, 223902 (2005).
[23] T. J. Kippenberg, H. Rokhsari, T. Carmon, A. Scherer, and K. J. Vahala, Phys. Rev. Lett. **95**, 033901 (2005).
[24] F. Marquardt, J. G. E. Harris, and S. M. Girvin, Phys. Rev. Lett. **96**, 103901 (2006).
[25] T. Corbitt *et al.*, Phys. Rev. A **74**, 021802 (2006).
[26] T. Carmon and K. J. Vahala, Phys. Rev. Lett. **98**, 123901 (2007).
[27] K. R. Brown, J. Britton, R. J. Epstein, J. Chiaverini, D. Leibfried, and D. J. Wineland, Phys. Rev. Lett. **99**, 137205 (2007).
[28] A. Naik *et al.*, Nature (London) **443**, 193 (2006).
[29] D. A. Rodrigues, J. Imbers, and A. D. Armour, Phys. Rev. Lett. **98**, 067204 (2007).
[30] D. A. Rodrigues, J. Imbers, T. J. Harvey, and A. D. Armour, New J. Phys. **9**, 84 (2007).
[31] K. W. Murch, K. L. Moore, S. Gupta, and D. M. Stamper-Kurn, Nature Phys. **4**, 561 (2008).
[32] H. Rokhsari, T. J. Kippenberg, T. Carmon, and K. J. Vahala, Opt. Express **13**, 5293 (2005).
[33] *xyz* positioner from attocube systems AG (Munich).
[34] I. Favero and K. Karrai, arXiv:0707.3117.
[35] M. Ludwig, B. Kubala, and F. Marquardt, arXiv:0803.3714.